PHOTONICS Research

Temperature dependence of the ionization coefficients of InAlAs and AlGaAs digital alloys

YUAN YUAN,[1] JIYUAN ZHENG,[1] YAOHUA TAN,[1] YIWEI PENG,[1] ANN-KATHRYN ROCKWELL,[2] SETH R. BANK,[2] AVIK GHOSH,[1] AND JOE C. CAMPBELL[1,*]

[1]Electrical and Computer Engineering Department, University of Virginia, 351 McCormick Rd., Charlottesville, Virginia 22904, USA
[2]Electrical and Computer Engineering Department, University of Texas at Austin, 1616 Guadalupe St., Austin, Texas 78758, USA
*Corresponding author: jccuva@virginia.edu

Received 17 April 2018; revised 1 June 2018; accepted 8 June 2018; posted 13 June 2018 (Doc. ID 328509); published 13 July 2018

Digital alloy $In_{0.52}Al_{0.48}As$ avalanche photodiodes exhibit lower excess noise than those fabricated from random alloys. This paper compares the temperature dependence, from 203 to 323 K, of the impact ionization characteristics of $In_{0.52}Al_{0.48}As$ and $Al_{0.74}Ga_{0.26}As$ digital and random alloys. These results provide insight into the low excess noise exhibited by some digital alloy materials, and these materials can even obtain lower excess noise at low temperature. © 2018 Chinese Laser Press

OCIS codes: (040.1345) Avalanche photodiodes (APDs); (260.3230) Ionization; (120.6780) Temperature; (230.5170) Photodiodes.

https://doi.org/10.1364/PRJ.6.000794

1. INTRODUCTION

Ionization coefficients are fundamental performance parameters for avalanche photodiodes (APDs), particularly the excess noise factor $F\langle M\rangle$ [1]. In the local-field model [2], the excess noise factor is expressed as $F\langle M\rangle = kM + (1-k)(2-1/M)$, where M is the multiplication gain and k is the ratio of the hole ionization coefficient, β, to the electron ionization coefficient, α. This model shows that the excess noise factor $F\langle M\rangle$ increases more slowly with gain for smaller values of k, which results in higher receiver sensitivity. Smaller k values also enable higher-gain-bandwidth products and, thus, operation at higher frequencies or bit rates [3].

Recently, $Al_xIn_{1-x}As_ySb_{1-y}$ digital alloy APDs have exhibited excess noise factors characterized by k as low as 0.01 [4–7]. In addition, $In_{0.52}Al_{0.48}As$ digital alloy APDs have achieved k values from 0.03 to 0.09, which are lower than those of the random alloy materials of the same composition [8–10]. However, other digital alloy materials, e.g., AlGaAs or InGaAs, do not exhibit lower noise compared with random alloy materials. It is well known that impact ionization in APDs is affected by temperature through the relation of the bandgap energy to the threshold energy, the phonon energy, and the phonon scattering mean free path [11–14]. In this work, we investigate the temperature dependence of impact ionization in two digital alloy materials, $In_{0.52}Al_{0.48}As$ (InAlAs in the following) and $Al_{0.74}Ga_{0.26}As$ (AlGaAs in the following), and compare them with random alloy InAlAs and AlGaAs APDs. The results provide insight into the variation in noise characteristics.

2. DEVICE STRUCTURE AND FABRICATION

All the wafers in this study are p-i-n structures grown by solid-source molecular beam epitaxy. A schematic cross section of the InAlAs APDs is shown in Fig. 1(a). The epitaxial layers are grown on n-type InP (001). A period of eight monolayers (ML) or 2.44 nm of the binary alloys InAs and AlAs is used to fabricate the InAlAs digital alloy [15]. The AlGaAs digital alloy APD is grown on an n-type GaAs (001) substrate. The period of the binary alloys AlAs and GaAs for the AlGaAs layers is 8.1 ML or 2.47 nm. A cross section of the AlGaAs APD is shown in Fig. 1(b).

The mesa-structure APDs were fabricated by standard photolithography. The InAlAs mesa-structure APDs were formed by wet etching in a 1:8:80 solution of H_2SO_4:H_2O_2:H_2O, and the AlGaAs mesas were etched in a 1:1:10 solution of H_3PO_4:H_2O_2:H_2O. Ti/Pt/Au was deposited as the top and bottom contacts by electron-beam evaporation. After lift-off of the metals, SU-8 was spun on the sidewall as a surface passivation.

3. EXPERIMENTS AND RESULTS

Excess noise measurements were carried out at room temperature using a He–Ne laser (543 nm) to ensure pure electron injection and an HP 8970 noise figure meter. Figure 2 shows the excess noise factor, $F\langle M\rangle$, of the InAlAs random and digital alloy APDs. The excess noise of the random alloy is characterized by a k value of 0.2, which is consistent with previous reports [8–10]. The k value for the digital alloy, on the other hand, is ~0.09.

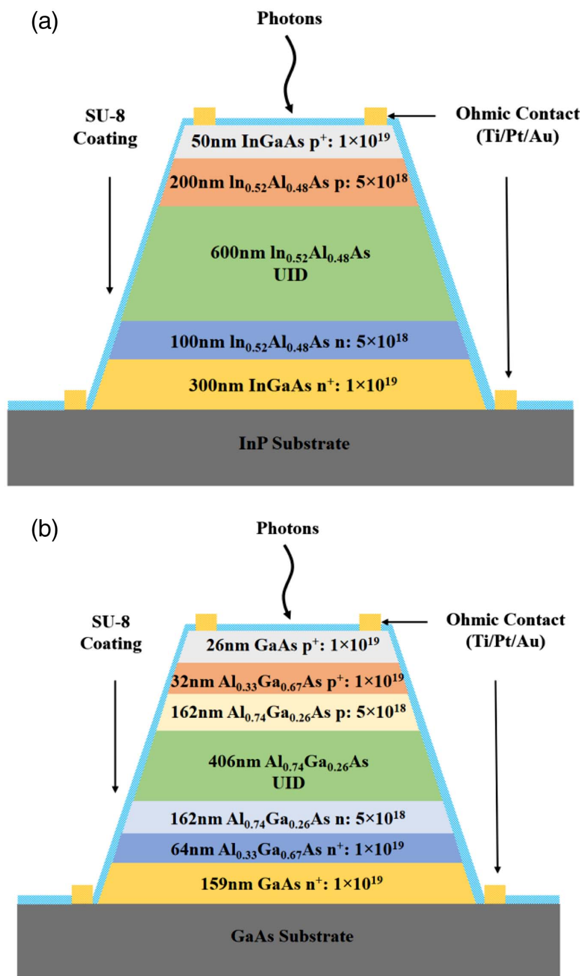

Fig. 1. Schematic cross sections of (a) InAlAs APDs and (b) AlGaAs APDs.

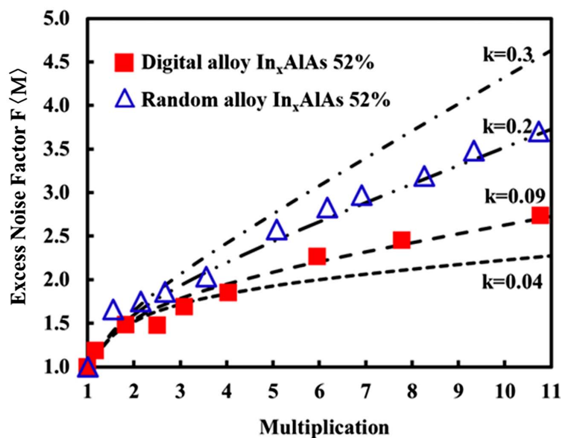

Fig. 2. Excess noise factor, $F\langle M\rangle$, of InAlAs digital and random alloy APDs.

The excess noises for the random alloy AlGaAs with Al concentration from 20% to 90% [16] and the digital alloy are shown in Fig. 3. As reported in Ref. [16], the excess noise of $Al_xGa_{1-x}As$ decreases with increasing Al concentration.

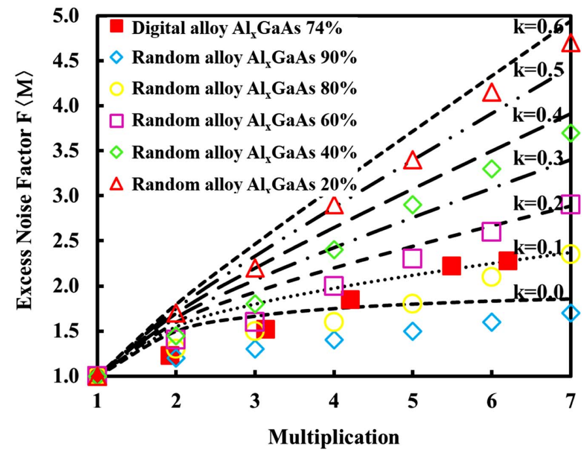

Fig. 3. Excess noise factor, $F\langle M\rangle$, of AlGaAs digital and random alloy APDs.

We note that the noise of the digital alloy with Al concentration ~74% (■) lies between the 60% (□) and 80% (○) random alloys. We conclude that the digital alloy does not suppress the noise in AlGaAs.

The band structures of digital and random alloys have been calculated using an environment-dependent tight binding model [17]. Figure 4(a) shows how the supercells were chosen for zinc-blende InAlAs. The supercell of the 8 ML digital alloy consists of 8 As, 4 In, and 4 Al atoms. Eight atoms comprise the random alloy supercell: 4 As, 2 In, and 2 Al atoms. In both structures, the In and Al compositions are 50%. Figure 4(b) illustrated the reciprocal space positions chosen to calculate band structures, where Γ is the center of the first Brillouin zone; A and D are the boundaries of the first Brillouin zone along the growth direction and an in-plane direction, respectively; B is a random point between Γ and D; and C and E are the boundaries of the first Brillouin zone of the B and D points along the growth direction.

It can be seen from Figs. 4(c) and 4(d) that there are significant differences in the band structures of the InAlAs random and digital alloys. At the first Brillouin zone boundary of the InAlAs digital alloy, there is a mini-gap between the second and third valance bands, while there are no gaps in the InAlAs random alloy.

In the conduction band of the InAlAs digital alloy, the electrons can gain energy through in-plane scattering; however, there are not equivalent paths for holes in the valence bands. Therefore, the valence band mini-gap can impede holes from achieving sufficient energy to initiate impact ionization, particularly at low temperature. As the temperature decreases, the probability of phonon scattering to a higher-order valence band is reduced, which will suppress the hole ionization coefficient, β. It follows that the k value and thus the excess noise factor of InAlAs digital alloys should decrease with decreasing temperature.

In order to verify this hypothesis, the excess noise was measured from 203 K (−70°C) to 323 K (50°C). In Fig. 5(a), the excess noise factor of the InAlAs random alloy is plotted at different temperatures. As shown in Fig. 5(b), the k value

is relatively independent of temperature and in the range 0.18–0.25, which is consistent with previous reports [8]. A fit to the temperature variation yields

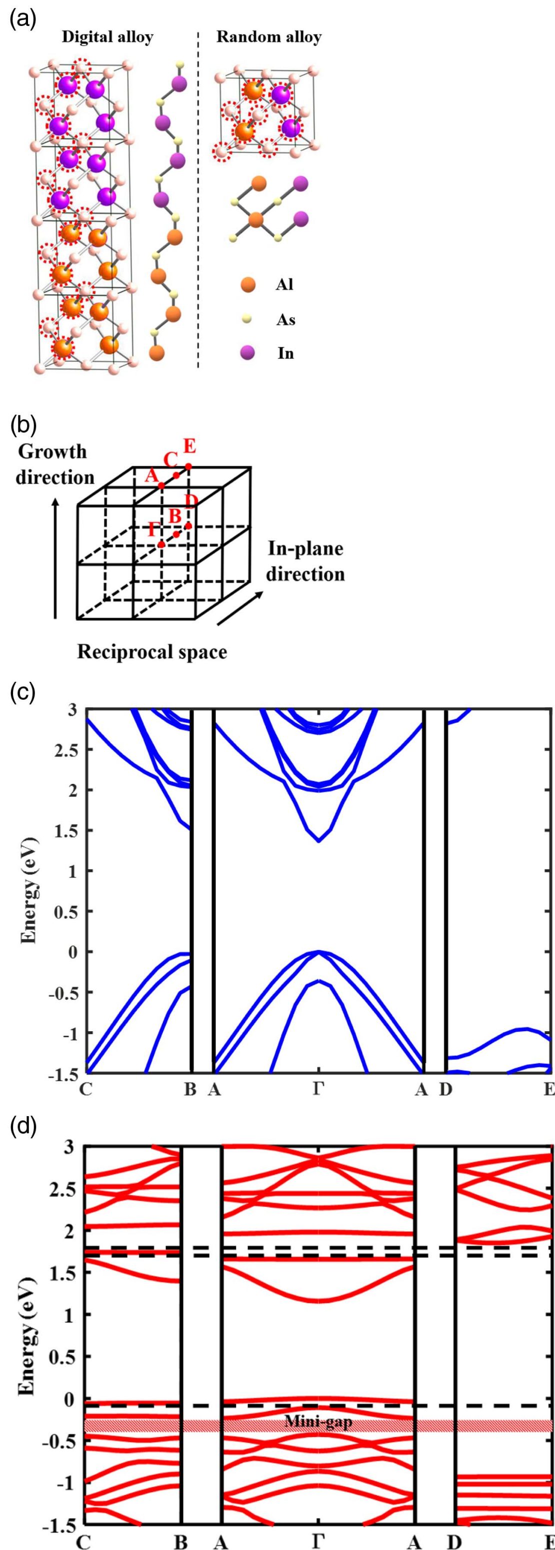

Fig. 4. (a) InAlAs digital and random alloy supercells, (b) positions in reciprocal space, (c) band structures of InAlAs random alloy at different positions, and (d) band structures of InAlAs digital alloy at different positions. The mini-gap in the valence band is marked.

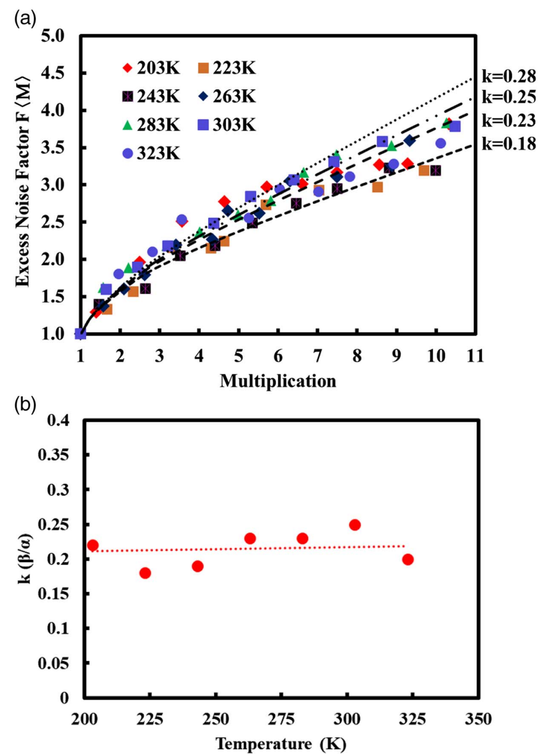

Fig. 5. Temperature dependence of (a) excess noise factor and (b) ionization coefficient ratio k for InAlAs random alloy APD.

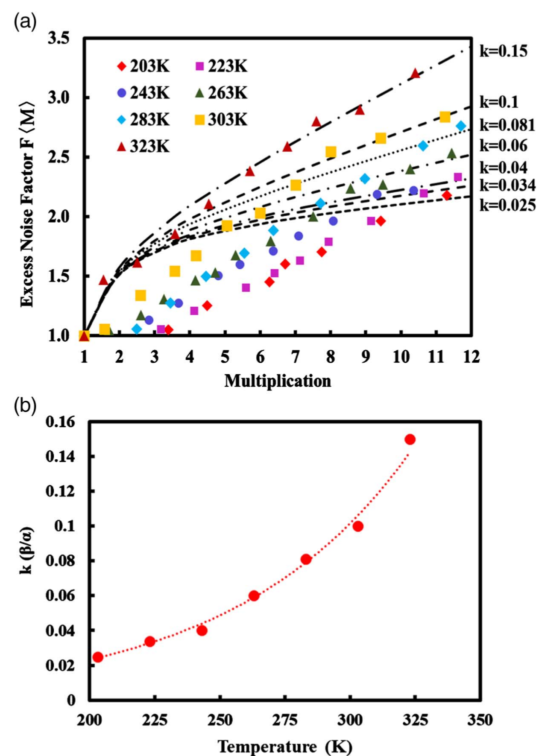

Fig. 6. Temperature dependence of (a) excess noise factor and (b) ionization coefficient ratio k for InAlAs digital alloy APD.

$$k = 0.2 + 6 \times 10^{-5} \times T \pm 0.04. \quad (1)$$

In contrast with the random alloy, the excess noise of the InAlAs digital alloy APDs exhibits strong temperature dependence, as shown in Fig. 6(a). This is reflected by the variation of the k value with temperature [Fig. 6(b)]; the k value increases exponentially with temperature and can be expressed as

$$k = 0.0012 \times \exp(0.0147 \times T). \quad (2)$$

The band structures of the AlGaAs random and digital alloys are shown in Figs. 7(a) and 7(b), respectively. The band structures are similar. Therefore, the AlGaAs random and digital alloys are expected to have similar excess noise performance. For the digital alloy, there are no mini-gaps; the highest energy of the third valance band is same as the lowest energy of the second valence band. This enables strong intraband scattering, which helps the holes to achieve higher energy. Thus, the impact ionization probability of holes in the AlGaAs digital alloy material is not projected to be strongly affected by temperature.

The excess noise of the AlGaAs APDs was measured from 203 K (−70°C) to 303 K (30°C). The excess noise of the digital alloy is plotted at different temperatures in Fig. 8(a). The results are similar to those for the InAlAs random alloy APD, i.e., the variation of excess noise with temperature is small. This is consistent with reported measurements on $Al_xGa_{1-x}As$ random

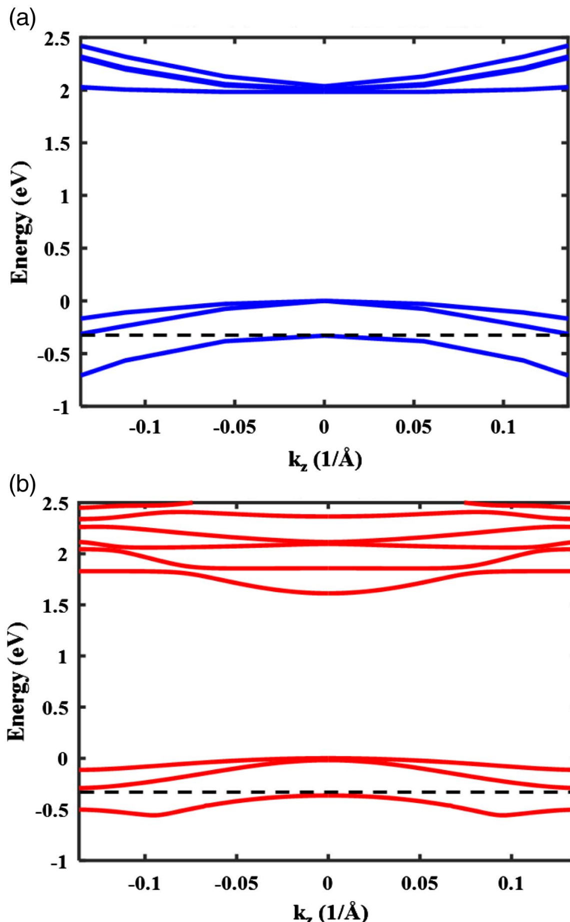

Fig. 7. Band structures of (a) AlGaAs random alloy and (b) AlGaAs digital alloy.

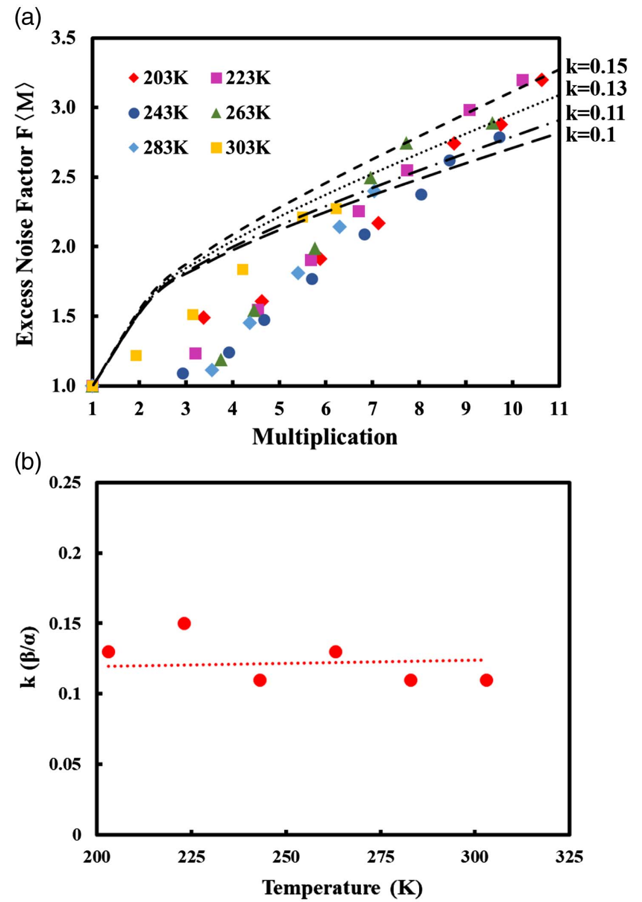

Fig. 8. Temperature dependence of (a) excess noise factor and (b) ionization coefficient ratio k for AlGaAs digital alloy p-i-n APD.

alloy APDs [18,19]. Figure 8(b) shows that as the temperature changes, k remains in the range 0.1–0.15 and obeys the relation

$$k = 0.11 + 5 \times 10^{-5} \times T \pm 0.04. \quad (3)$$

4. CALCULATIONS AND DISCUSSION

The multiplication gain for pure electron injection, M_e, can be expressed as [20]

$$M_e = \left\{1 - \int_0^W \alpha \exp\left[-\int_0^x (\alpha - \beta)\mathrm{d}x'\right]\mathrm{d}x\right\}^{-1}, \quad (4)$$

where W is the thickness of the multiplication region. For a uniform electric field, the ionization coefficients are given by the following expressions:

$$\alpha = \frac{\ln[k - (k-1)/M_e]}{(k-1)W}, \quad (5)$$

$$\beta = k \cdot \alpha. \quad (6)$$

Using these expressions, the ionization coefficients can be determined from the gain versus voltage curves at different temperatures. The relation between electric field and gain is obtained from photocurrent versus bias measurements. Figures 9(a), 9(b), and 9(c) show the ionization coefficients

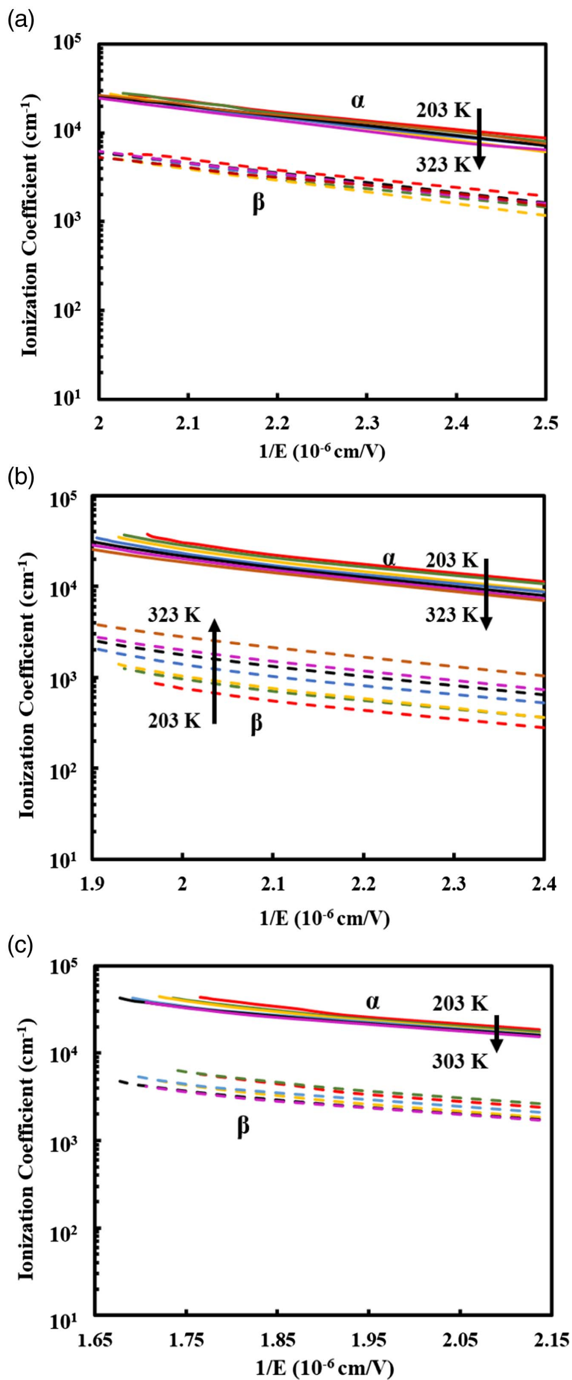

Fig. 9. Ionization coefficients of (a) InAlAs random alloy, (b) InAlAs digital alloy, and (c) AlGaAs digital alloy at different temperatures.

versus the inverse electric field, $1/E$, at different temperatures for InAlAs random, InAlAs digital, and AlGaAs digital alloys, respectively.

In all three plots, the electron ionization coefficients exhibit modest decreases with temperature, owing to increased phonon scattering. However, the most significant change is that of the hole ionization coefficient in the InAlAs digital alloy, which decreases with decreasing temperature. This is due primarily

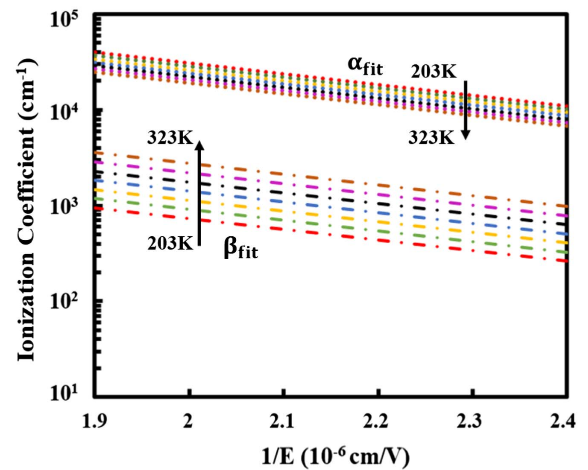

Fig. 10. Plots of Eqs. (7) and (8), the temperature-dependent ionization coefficients of the InAlAs digital alloy.

to the presence of the mini-gap in the valence band and explains the reduction in k and excess noise with decreasing temperature.

By fitting the experimental ionization coefficients of the InAlAs digital alloy, the relationships among temperature T, electric field E, and the ionization coefficients can be expressed by the following equations, and they are plotted in Fig. 10:

$$\alpha(T, E) = 2.2 \times 10^7 \times \exp\left[-0.004 \times T - \left(\frac{3.5 \times 10^6}{E}\right)^{0.9}\right], \tag{7}$$

$$\beta(T, E) = 2.5 \times 10^4 \times \exp\left[0.011 \times T - \left(\frac{3.5 \times 10^6}{E}\right)^{0.9}\right]. \tag{8}$$

5. CONCLUSION

The ionization characteristics of InAlAs random alloy, InAlAs digital alloy, and AlGaAs digital alloy have been investigated at different temperatures. The k values of the InAlAs digital alloy APDs decrease exponentially with decreasing temperature, owing to the suppression of hole ionization, which in turn is due to a mini-gap in the valence band. The experimental results are consistent with the simulated band structures and provide insight into the low excess noise exhibited by the InAlAs digital alloy and the absence of noise suppression in the AlGaAs digital alloy.

Funding. Defense Advanced Research Projects Agency (DARPA) (W911NF-10-1-0391); Army Research Office (ARO) (W911NF-10-1-0391).

REFERENCES

1. J. C. Campbell, "Recent advances in avalanche photodiodes," J. Lightwave Technol. **34**, 278–285 (2016).

2. R. J. McIntyre, “Multiplication noise in uniform avalanche photodiodes,” IEEE Trans. Electron. Devices **ED-13**, 164–168 (1966).
3. R. B. Emmons, “Avalanche-photodiode frequency response,” J. Appl. Phys. **38**, 3705–3714 (1967).
4. M. E. Woodson, M. Ren, S. J. Maddox, Y. Chen, S. R. Bank, and J. C. Campbell, “Low-noise AlInAsSb avalanche photodiode,” Appl. Phys. Lett. **108**, 081102 (2016).
5. M. Ren, S. J. Maddox, M. E. Woodson, Y. Chen, S. R. Bank, and J. C. Campbell, “AlInAsSb separate absorption, charge, and multiplication avalanche photodiodes,” Appl. Phys. Lett. **108**, 191108 (2016).
6. M. Ren, S. J. Maddox, M. E. Woodson, Y. Chen, S. R. Bank, and J. C. Campbell, “Low excess noise $Al_xIn_{1-x}As_ySb_{1-y}$ (x: 0.3–0.7) avalanche photodiodes,” in *Conference on Lasers and Electro-Optics (CLEO)* (IEEE, 2016), paper STh1G.1.
7. A. K. Rockwell, Y. Yuan, A. H. Jones, S. D. March, S. R. Bank, and J. C. Campbell, “$Al_{0.8}In_{0.2}As_{0.23}Sb_{0.77}$ avalanche photodiodes,” IEEE Photon. Technol. Lett. **30**, 1048–1051 (2018).
8. C. Lenox, P. Yuan, H. Nie, O. Baklenov, C. Hansing, J. C. Campbell, A. L. Holmes, Jr., and B. G. Streetman, “Thin multiplication region InAlAs homojunction avalanche photodiodes,” Appl. Phys. Lett. **73**, 783–784 (1998).
9. Y. L. Goh, A. R. J. Marshall, D. J. Massey, J. S. Ng, C. H. Tan, M. Hopkinson, J. P. R. David, S. K. Jones, C. C. Button, and S. M. Pinches, “Excess avalanche noise in $In_{0.52}Al_{0.48}As$,” IEEE J. Quantum Electron. **43**, 503–507 (2007).
10. N. Li, R. Sidhu, X. Li, F. Ma, X. Zheng, S. Wang, G. Karve, S. Demiguel, A. L. Holmes, Jr., and J. C. Campbell, “InGaAs/InAlAs avalanche photodiode with undepleted absorber,” Appl. Phys. Lett. **82**, 2175–2177 (2003).
11. F. Capasso, R. E. Nahory, M. A. Pollack, and T. P. Pearsall, “Observation of electronic band-structure effects on impact ionization by temperature tuning,” Phys. Rev. Lett. **39**, 723–726 (1977).
12. F. Osaka and T. Mikawa, “Low-temperature characteristics of electron ionization rates in (100)- and (111)-oriented InP,” J. Appl. Phys. **58**, 4426–4430 (1985).
13. K. Taguchi, T. Torikai, Y. Sugimoto, K. Makita, and H. Ishihara, “Temperature dependence of impact ionization coefficients in InP,” J. Appl. Phys. **59**, 476–481 (1986).
14. D. J. Massey, J. P. R. David, and G. J. Rees, “Temperature dependence of impact ionization in submicrometer silicon devices,” IEEE Trans. Electron. Dev. **53**, 2328–2334 (2006).
15. S. J. Maddox, S. D. March, and S. R. Bank, “Broadly tunable AlInAsSb digital alloys grown on GaSb,” Cryst. Growth Des. **16**, 3582–3586 (2016).
16. X. G. Zheng, “Long-wavelength, high-speed avalanche photodiodes and APD arrays,” Ph.D. dissertation (University of Texas at Austin, 2004).
17. Y. Tan, M. Povolotskyi, T. Kubis, T. B. Boykin, and G. Klimeck, “Transferable tight-binding model for strained group IV and III-V materials and heterostructures,” Phys. Rev. B **94**, 045311 (2016).
18. X. G. Zheng, P. Yuan, X. Sun, G. S. Kinsey, A. L. Holmes, B. G. Streetman, and J. C. Campbell, “Temperature dependence of the ionization coefficients of $Al_xGa_{1-x}As$,” IEEE J. Quantum Electron. **36**, 1168–1173 (2000).
19. C. N. Harrison, J. P. R. David, M. Hopkinson, and G. J. Rees, “Temperature dependence of avalanche multiplication in submicron $Al_{0.6}Ga_{0.4}As$ diodes,” J. Appl. Phys. **92**, 7684–7686 (2002).
20. F. Capasso, “Physics of avalanche photodiodes,” Semicond. Semimetals **22**, 1–172 (1985).